Journal of Hepatocellular Carcinoma

Dovepress
Taylor & Francis Group

Open Access Full Text Article

ORIGINAL RESEARCH

C/EBP-β Mediates the Reversal of Sorafenib Resistance by Tunicamycin in Hepatocellular Carcinoma

Chong Pang[1,2,*], Jian Chen[3,*], Mingyi Chu[4], Jianshuang Chen[1], Han Wang[1], Hao Miao[1]

[1]Functional Experiment Center, School of Basic Medicine Sciences, Chengde Medical University, Chengde, Hebei, People's Republic of China; [2]Hebei Key Laboratory of Nerve Injury and Repair, Chengde Medical University, Chengde, Hebei, People's Republic of China; [3]Digestive System Department, Affiliated Hospital of Chengde Medical University, Chengde Medical University, Chengde, Hebei, People's Republic of China; [4]Institute of Sericulture, Chengde Medical University, Chengde, Hebei, People's Republic of China

*These authors contributed equally to this work

Correspondence: Hao Miao, Functional Experiment Center, School of Basic Medicine Sciences, Chengde Medical University, Chengde, Hebei, People's Republic of China, Email miaohao_1986@cdmc.edu.cn

Introduction: The multikinase inhibitor sorafenib is a standard-of-care therapy for advanced hepatocellular carcinoma (HCC). However, acquired resistance to sorafenib severely compromises its long-term clinical efficacy. This study aimed to investigate whether the endoplasmic reticulum (ER) stress inducer tunicamycin (TM) could overcome this resistance and to elucidate the central role of the transcription factor CCAAT/enhancer-binding protein β (C/EBP-β) in this process.

Methods: We established sorafenib-resistant hepatocellular carcinoma HepG2 and Huh7 cell lines to mimic the resistant phenotype. The sensitizing effect of TM was evaluated by assessing proliferation, colony formation, reactive oxygen species (ROS) production, and apoptosis. Therapeutic efficacy was further validated in vivo using subcutaneous and orthotopic xenograft models.

Results: We found that TM significantly inhibited the proliferation and clonogenicity of sorafenib-resistant cells. TM treatment upregulated C/EBP-β expression and restored sensitivity to sorafenib. Mechanistically, C/EBP-β overexpression phenocopied the effect of TM, whereas its knockdown attenuated TM-induced sensitization. Furthermore, TM induced a C/EBP-β-dependent increase in intracellular ROS, triggering the intrinsic apoptotic pathway characterized by p53 accumulation, an increased Bax/Bcl-2 ratio, and caspase-3 cleavage. In vivo, the combination of TM and C/EBP-β overexpression exerted potent antitumor effects, reducing tumor volume by approximately 91% relative to the sorafenib-only control group in subcutaneous models.

Conclusion: Our study identified C/EBP-β as a key effector of the terminal pro-apoptotic ER stress response. While the direct clinical application of TM is limited by its systemic toxicity, these findings highlight the clinical translational potential of targeting the ER stress-C/EBP-β axis, offering a novel combination therapeutic strategy for patients with acquired sorafenib resistance.

Keywords: hepatocellular carcinoma, HCC, sorafenib-resistance, endoplasmic reticulum, ER stress, tunicamycin, C/EBP-β, reactive oxygen species, ROS

Introduction

Hepatocellular carcinoma (HCC) ranks as the fourth leading cause of cancer-related mortality worldwide, characterized by high incidence and poor prognosis. For patients with advanced-stage disease, the multikinase inhibitor sorafenib has long served as the standard of care. By blocking multiple intracellular kinases, including VEGFR, PDGFR, and Raf family kinases, sorafenib effectively suppresses tumor angiogenesis and cell proliferation, conferring significant survival benefits.[1] However, the clinical efficacy of sorafenib is often severely compromised by acquired resistance, representing the primary obstacle to durable therapeutic responses.[2] HCC cells develop sorafenib resistance through multifaceted mechanisms, including epigenetic reprogramming, remodeling of the tumor microenvironment, and evasion of regulated cell death pathways such as ferroptosis.[3,4] Given this complexity, overcoming resistance is crucial for improving patient

https://doi.org/10.2147/JHC.S587037
Received: 16 December 2025
Accepted: 27 March 2026
Published: 13 April 2026

outcomes. Consequently, there is an urgent need to identify potent sorafenib sensitizers that can abrogate these resistant phenotypes.

The role of the cellular stress response, particularly endoplasmic reticulum (ER) stress, in sorafenib resistance has garnered increasing attention.[5,6] While adaptive ER stress promotes survival, persistent or unresolved ER stress is known to trigger apoptosis, a principle increasingly exploited in anti-cancer strategies.[7,8] The transcription factor CCAAT/enhancer-binding protein β (C/EBP-β) acts as a downstream effector of the ER stress pathway.[9] Although C/EBP-β functions can be context-dependent—often influenced by the ratio of its activating (LAP) and inhibitory (LIP) isoforms—it generally functions as a key regulator of cell fate under stress conditions.[10] Previously, we reported that in hepatoblastoma, C/EBP-β works synergistically with sorafenib to exert potent anti-tumor activity.[11] However, it remains unclear whether the ER stress pathway can be therapeutically leveraged to modulate C/EBP-β expression and thereby reverse acquired sorafenib resistance in HCC.

To induce robust ER stress, we utilized Tunicamycin (TM), a naturally occurring antibiotic that specifically inhibits the first step of N-linked glycosylation. By preventing proper protein folding, TM acts as a classic and highly potent pharmacological inducer of severe ER stress. Compared to other ER stress inducers (such as thapsigargin or bortezomib), TM was selected for this study due to its distinct ability to profoundly activate the terminal unfolded protein response (UPR) and upregulate C/EBP-β.[12]

Therefore, in this study, we aimed to systematically investigate the therapeutic potential of TM in HCC. We characterized the specific dysregulation of C/EBP-β expression in sorafenib-resistant HCC cells, determined whether TM could effectively reverse sorafenib resistance, and tested whether this resensitization functionally depends on a C/EBP-β-driven reactive oxygen species (ROS) apoptotic axis. Finally, we validated the clinical relevance of the TM and C/EBP-β combination strategy using in vivo xenograft models, aiming to provide a novel mechanistic framework for restoring chemosensitivity in drug-resistant HCC.

Materials and Methods

Cell Lines, Culture Conditions, and Reagents

Human hepatocellular carcinoma (HCC) cell lines HepG2 and Huh7 were obtained from the Cell Bank of the Institute of Biochemistry and Cell Biology, Chinese Academy of Sciences (Shanghai, China). Sorafenib-resistant (SR) cell lines HepG2-R was purchased from Zhejiang Meisen Cell Technology Co., Ltd. (China). The Huh7-R subline was established by exposing parental Huh7 cells to stepwise increasing concentrations of sorafenib (from 0.5 to 4 μM) over a period of 6 months. Resistance stability was verified by determining the IC_{50} after 5 drug-free passages. All cell lines were maintained in Dulbecco's Modified Eagle's Medium (DMEM) (Servicebio, China) supplemented with 10% fetal bovine serum (Gibco, USA), 100 U/mL penicillin, and 100 μg/mL streptomycin. Cells were cultured at 37 °C in a humidified incubator containing 5% CO_2. To maintain drug resistance, SR cell lines were continuously cultured in medium containing sorafenib at a concentration of 4 μM.

Sorafenib (SJ-MX0071A, SparkJade, China), tunicamycin (TM; T101151, Aladdin, China), and N-acetylcysteine (NAC; A105422, Aladdin, China) were dissolved in dimethyl sulfoxide (DMSO) or sterile water (for NAC) to prepare stock solutions and stored at −20 °C. The final concentration of DMSO in all in vitro assays was strictly maintained below 0.1% (v/v), and control groups were treated with an equivalent volume of DMSO vehicle to exclude solvent-induced cytotoxicity. The following primary antibodies were used for Western blot and immunohistochemistry: C/EBP-β (A0711, Abclonal, China), p53 (ET1601-13, HUABIO, China), Bax (ET1603-34, HUABIO, China), Bcl-2 (ET1702-53, HUABIO, China), Cleaved Caspase-3 (ET1602-47, HUABIO, China), GAPDH (K200102M, Solarbio, China), and Ki-67 (PT0321R, Immunoway, China).

Cell Viability and IC_{50} Assay

Cell viability was evaluated using the Cell Counting Kit-8 (CCK-8; Dojindo, Kumamoto, Japan) according to the manufacturer's instructions. Briefly, cells were seeded in 96-well plates at a density of 1×10^4 cells/well and allowed to adhere overnight. Subsequently, cells were treated with various concentrations of sorafenib, tunicamycin (TM), or their

combination for 48 h. Following the treatment period, 10 μL of CCK-8 solution was added to each well, and the plates were incubated for an additional 1 h at 37 °C. The optical density (OD) was measured at 450 nm using a microplate reader (Bio-Rad Laboratories, USA). Dose-response curves were plotted and half-maximal inhibitory concentration (IC_{50}) values were calculated using a nonlinear regression model in GraphPad Prism 9.5.

Colony Formation Assay

For the colony formation assay, the cells were seeded in 6-well plates at a density of 500 cells/well. After an overnight incubation to allow for attachment, the culture medium was replaced with fresh medium containing either sorafenib (8 μM) alone or sorafenib in combination with increasing concentrations of TM (2, 4, and 8 μM) for 48 h. Then, the cells were cultured for 14 days, after which the colonies were washed with phosphate-buffered saline (PBS), fixed with 4% paraformaldehyde for 15 min, and stained with 0.1% crystal violet for 20 min. After rinsing with water and air-drying, the plates were photographed. The total number of visible colonies was quantified using ImageJ software.

RNA Extraction and Real-Time Quantitative PCR (RT-qPCR)

Total RNA was extracted from cultured cells using the TRIzol reagent (Invitrogen, USA) according to the manufacturer's protocol. The concentration and purity of the RNA were determined using a NanoDrop 2000 spectrophotometer (Thermo Fisher Scientific, USA), ensuring an A260/A280 ratio between 1.8 and 2.0. Subsequently, 1 μg of total RNA was reverse-transcribed into cDNA using the PrimeScript RT Reagent Kit with gDNA Eraser (Takara, Japan). RT-qPCR was conducted on an ABI 7500 Real-Time PCR System (Applied Biosystems, USA) using TB Green Premix Ex Taq II (Takara, Japan). All primers were synthesized and purified via ULTRAPAGE technology by Sangon Biotech (Shanghai) Co., Ltd. The PCR cycling protocol was as follows: initial denaturation at 95 °C for 30s, followed by 40 cycles of denaturation at 95 °C for 5s and annealing/extension at 60 °C for 34s. The relative mRNA expression of C/EBP-β was calculated using the $2^{-\Delta\Delta Ct}$ method. GAPDH stability across treatment groups was validated, confirming its suitability as an endogenous reference gene. The primer sequences used were as follows: *C/EBP-β* forward: 5′-AAGCACAGCGACGAGTACAA-3′ and *C/EBP-β* reverse: 5′-TGCTCCACCTTCTTCTGCAG-3′; *GAPDH* Forward: 5′-GCACCGTCAAGGCTGAGAAC-3′ and *GAPDH* Reverse: 5′-TGGTGAAGACGCCAGTGGA-3′.

Western Blot Analysis

Cells were harvested and lysed on ice in RIPA buffer (Beyotime, China) supplemented with a protease and phosphatase inhibitor cocktail (PMSF). Total protein concentration in the lysates was quantified using a BCA Protein Assay Kit (Thermo Fisher Scientific, USA) to ensure equal loading. For each sample, 30 μg of total protein was separated on a 10% SDS-PAGE gel and transferred to PVDF membranes (Solarbio, China). Membranes were blocked for 2 h at room temperature in 5% non-fat milk prepared in Tris-buffered saline containing 0.1% Tween 20 (TBST). Primary antibodies were diluted as recommended by the manufacturer and incubated overnight at 4°C with gentle shaking. After washing, membranes were incubated with HRP-conjugated secondary antibodies (1:5000 dilution) for 1 h at room temperature. Protein bands were visualized using an enhanced chemiluminescence (ECL) detection reagent (Solarbio, China) and the signal was captured using the Odyssey Infrared Imaging System (LI-COR Biosciences, USA).

Plasmid Transfection and Lentiviral Transduction

For transient knockdown of C/EBP-β, cells were transfected with an shRNA-expressing plasmid targeting the sequence 5′-CGACTTCCTCTCCGACCTCTT-3′ (General Biosystems, China) using Lipofectamine 3000 (Invitrogen). For transient overexpression, pcDNA3.1-C/EBP-β-3 × Flag vector was used. A stable C/EBP-β-overexpressing (C/EBP-β-oe) Huh7-R cell line was generated by transduction with GV492 lentivirus encoding C/EBP-β (Genechem, China), followed by selection with puromycin (2.5 μg/mL). The expression was confirmed by Western blotting.

In vivo Xenograft Tumor Model

All animal experiments were approved by the Chengde Medical College Animal Care and Use Committee (Approval No. CDMULAC-20241104-051) and were conducted in strict accordance with the guidelines for the care and use of laboratory animals. 4-week-old male BALB/c nude mice (16–18 g) were purchased from Beijing HFK Bioscience Co., Ltd. (China) and housed under specific pathogen-free (SPF) conditions. Two types of xenograft models were established using Huh7-R cells to evaluate tumor growth in vivo. For the subcutaneous xenograft model, Huh7-R cells or stable C/EBP-β-oe Huh7-R cells (5×10^6 in 100μL PBS per mouse) were subcutaneously injected into the right upper flank. Moreover, to mimic the liver microenvironment, an orthotopic model was established via surgical implantation of tumor fragments. Briefly, subcutaneous tumors formed by Huh7-R or C/EBP-β-oe Huh7-R cells were harvested when they reached approximately 500 mm^3, cut into uniform 1–2 mm^3 fragments, and surgically implanted into the left lateral liver lobe of recipient mice under general anesthesia induced by isoflurane inhalation. Two weeks after cell implantation, mice were randomized based on their baseline tumor volumes into four groups (n=6/group) to ensure uniform tumor burden across groups: (1) sorafenib group (control), mice bearing Huh7-R tumors treated with sorafenib alone; (2) TM group, mice bearing Huh7-R tumors treated with sorafenib + TM; (3) C/EBP-β-oe group, mice bearing C/EBP-β-overexpressing Huh7-R tumors treated with sorafenib alone; (4) TM + C/EBP-β-oe group, mice bearing C/EBP-β-overexpressing Huh7-R tumors treated with sorafenib + TM. All groups received a baseline treatment of sorafenib (15 mg/kg/day by oral gavage). The TM and TM + C/EBP-β-oe groups received additional TM (0.04 mg/kg/day, by intraperitoneal injection). Tumor volume ($V = 0.5 \times \text{length} \times \text{width}^2$) was measured every two days. After 38 days, the mice were euthanized by CO_2 overdose (inhalation) in accordance with the American Veterinary Medical Association (AVMA) Guidelines for the Euthanasia of Animals, and the tumors were excised for weighing and histological analysis.

Histological and Immunohistochemical (IHC) Analyses

Excised tumor tissues were fixed in 4% paraformaldehyde, embedded in paraffin, and cut into 4–5 μm thick sections. Hematoxylin and eosin (H&E) staining was performed according to standard protocols to evaluate pathological changes and cellular morphology. For IHC analysis, paraffin sections were deparaffinized in xylene and rehydrated through a graded ethanol series. Antigen retrieval was performed by heating the sections in boiling 0.01 M sodium citrate buffer (pH 6.0) for 2 min. To inhibit endogenous peroxidase activity, sections were incubated with 3% hydrogen peroxide for 10 min at room temperature. Subsequently, non-specific binding was blocked with 10% normal goat serum for 1 h. The sections were then incubated overnight at 4 °C with primary antibodies against C/EBP-β (1:200) or Ki-67 (1:200). Following three washes with PBS, slides were incubated with HRP-conjugated secondary antibodies for 1 h at room temperature. Immunoreactivity was visualized using a 3,3′-diaminobenzidine (DAB) substrate kit. The reaction was monitored microscopically and terminated with water upon optimal color development. Finally, sections were counterstained with hematoxylin, dehydrated, and mounted with neutral resin. Staining patterns were semi-quantitatively scored by two independent pathologists who were blinded to the treatment groups. The scoring system integrated both staining intensity (0, negative; 1, weak; 2, moderate; 3, strong) and the percentage of positive cells (0, <5%; 1, 5–25%; 2, 26–50%; 3, 51–75%; 4, >75%). An immunoreactivity score (IRS) was calculated by multiplying the intensity score by the percentage score, resulting in a range of 0 to 12. Any discrepancies in scoring were resolved through discussion and consensus between the pathologists.

Measurement of Reactive Oxygen Species (ROS)

Intracellular ROS levels were measured using a DCFDA/H2DCFDA - Cellular ROS Assay Kit (ab113851, Abcam, UK). Cells were treated as indicated, washed with assay buffer, and then incubated with 20 μM DCFDA solution for 45 min at 37 °C. After washing, fluorescence images were captured using a fluorescence microscope (excitation/emission = 485/535 nm). The mean fluorescence intensity per cell was quantified using the ImageJ software.

TUNEL Assay

According to the manufacturer's instructions, the apoptotic cells were determined by TUNEL staining using a One Step TUNEL Apoptosis Assay Kit (Beyotime, Jiangsu, China), and the nuclei were stained with DAPI. Images were captured

using an Olympus microscope at 540 nm excitation and 560 nm emission wavelengths. TUNEL-positive nuclei (green fluorescence) were counted in 10 random fields (×200) and then averaged.

Statistical Analysis

All in vitro experiments were conducted independently at least three times. Data are presented as the mean ± standard deviation (SD). Statistical analyses were performed using GraphPad Prism 9.5 software. Comparisons between two groups were performed using two-tailed Student's *t*-test. For comparisons among multiple groups, one-way analysis of variance (ANOVA) followed by Tukey's post-hoc test was used. A *P-value* (*P*) less than 0.05. The significance levels are denoted in the figures as follows: $P < 0.05$ (*), $P < 0.01$ (**) and $P < 0.001$ (***).

Results

Reduced C/EBP-β Expression Characterizes the Acquired Sorafenib-Resistant Phenotype in HCC

To investigate the mechanisms underlying acquired resistance, we first characterized the drug sensitivity profiles of parental versus sorafenib-resistant (SR) HCC cell models. Using the CCK-8 cell viability assay, we determined the half-maximal inhibitory concentration (IC_{50}) for each line. As depicted in Figure 1A, SR sublines exhibited a marked reduction in sorafenib sensitivity. Specifically, the IC_{50} values increased by 4.04-fold in HepG2-R cells (32.71 μM vs. 8.09 μM) and 3.69-fold in Huh7-R cells (23.48 μM vs. 6.37 μM) compared to their respective parental counterparts. Crucially, the stability of this resistant phenotype was validated, as IC_{50} values for both HepG2-R and Huh7-R cells remained statistically unchanged after 5 continuous passages in drug-free medium (data not shown), confirming the establishment of robustly stable resistant lines. We next examined whether this resistance correlated with alterations in C/EBP-β expression. RT-qPCR and Western blot analyses revealed a significant downregulation of C/EBP-β mRNA and protein in both SR lines (Figure 1B). Notably, despite potential baseline genetic differences between HepG2 and Huh7 cells, both cell lines converged on this shared phenotype of C/EBP-β suppression upon acquiring drug resistance. To establish a causal link, we silenced C/EBP-β in parental Huh7-R cells using specific shRNA (knockdown efficiency confirmed in Figure S1A) Functional assays demonstrated that C/EBP-β knockdown significantly attenuated sorafenib-induced growth inhibition and clonogenic suppression (Figure S1B and C), thereby phenocopying the resistant state.

Tunicamycin Synergistically Reverses Sorafenib Resistance in a C/EBP-β-Dependent Manner

Based on the inverse correlation between C/EBP-β expression and sorafenib resistance, we postulated that restoring C/EBP-β via ER stress induction could resensitize resistant cells. We evaluated the therapeutic potential of tunicamycin (TM). TM treatment elicited a dose-dependent upregulation of C/EBP-β at both protein and mRNA levels in Huh7-R cells (Figure 2A and B). Functionally, CCK-8 and colony formation assays demonstrated that TM synergistically potentiated the cytotoxicity of sorafenib, markedly suppressing cell viability and clonogenic potential in Huh7-R cells (Figure 2C and D). Specifically, while resistant cells could easily evade the growth-inhibitory effects of sorafenib monotherapy, the addition of TM triggered severe ER stress that dismantled their adaptive survival mechanisms, thereby restoring their susceptibility to sorafenib. To mechanistically validate this dependency, we performed gain- and loss-of-function studies (Figure 2E). Direct overexpression of C/EBP-β (C/EBP-β-oe) was sufficient to restore sorafenib sensitivity, significantly reducing cell viability and colony formation across both Huh7-R and HepG2-R models (Figure 2F–I). Conversely, shRNA-mediated knockdown of C/EBP-β (shC/EBP-β) significantly abrogated the sensitizing effects of TM, partially rescuing cell survival and highlighting C/EBP-β as a critical node in TM-mediated resensitization.

Tunicamycin and C/EBP-β Overexpression Cooperatively Suppress Sorafenib-Resistant Tumor Growth in vivo

To translate our findings in vivo, we utilized subcutaneous and orthotopic xenograft models. Since the primary objective of this study was to investigate the reversal of acquired resistance to sorafenib rather than evaluating TM as a standalone

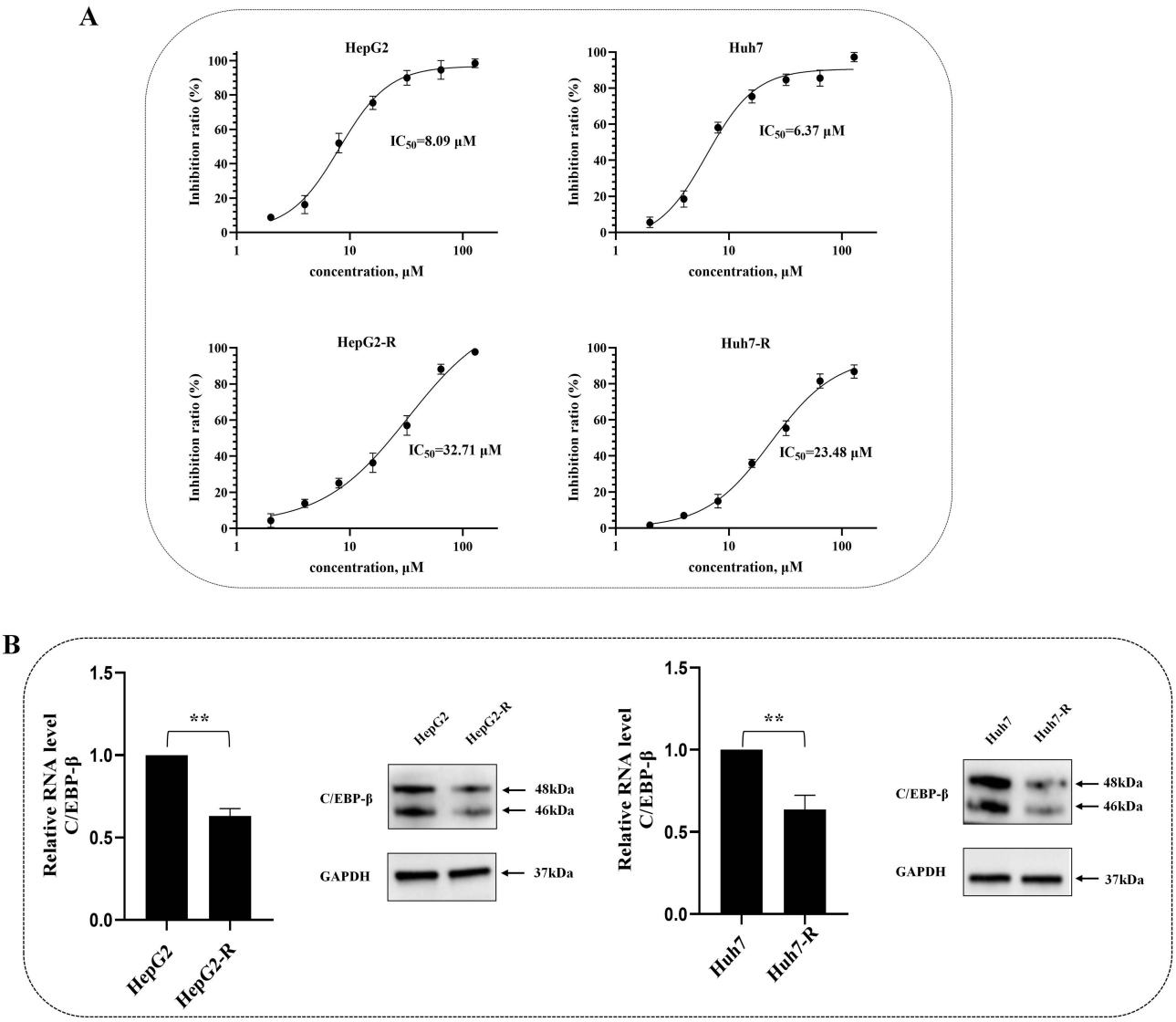

Figure 1 C/EBP-β is downregulated in sorafenib-resistant hepatocellular carcinoma cells. (**A**) The inhibition ratio (%) of parental (HepG2, Huh7) and sorafenib-resistant (HepG2-R, Huh7-R) HCC cells was measured by CCK-8 assay after treatment with a gradient of sorafenib concentrations for 48 h. The calculated IC_{50} values are indicated on the dose-response curves. Data are presented as mean ± SD (n=3). (**B**) The relative mRNA and protein expression levels of C/EBP-β in parental and sorafenib-resistant cell lines were determined by RT-qPCR (bar graphs) and Western blot (gel images), respectively. GAPDH was used as an internal control. Data in the bar graphs are presented as mean ± SD from three independent experiments. $^{**}P < 0.01$ compared to the corresponding parental cells.

first-line therapy, all animal groups were maintained on a baseline sorafenib regimen to mimic the clinical scenario of a patient failing sorafenib therapy. We then assessed the additive benefits of TM treatment and C/EBP-β overexpression. In the subcutaneous Huh7-R model, repeated measures ANOVA statistical evaluation of tumor growth kinetics (Figure 3B) revealed significant therapeutic divergence starting from Day 22. The dual combination group (TM + C/EBP-β-oe) exhibited the most profound synergistic tumor suppression, reducing tumor volume by 91% relative to the sorafenib-only control group by Day 38 (Figure 3A and B). Morphological assessment via H&E staining confirmed extensive necrotic regions in the treatment groups, particularly in the dual-combination cohort (Figure 3C). Objective semi-quantitative IHC analysis using the Immunoreactivity Score (IRS) further corroborated that therapeutic efficacy correlated with significantly restored C/EBP-β expression and a significant reduction in the proliferation marker Ki-67 (Figures 3D and S2). Furthermore, in the liver microenvironment-mimicking orthotopic model, the combination treatment significantly alleviated the hepatic tumor burden and preserved normal hepatic parenchyma architecture, with only minimal residual tumor foci observed in the dual-therapy group (Figure 3E and F).

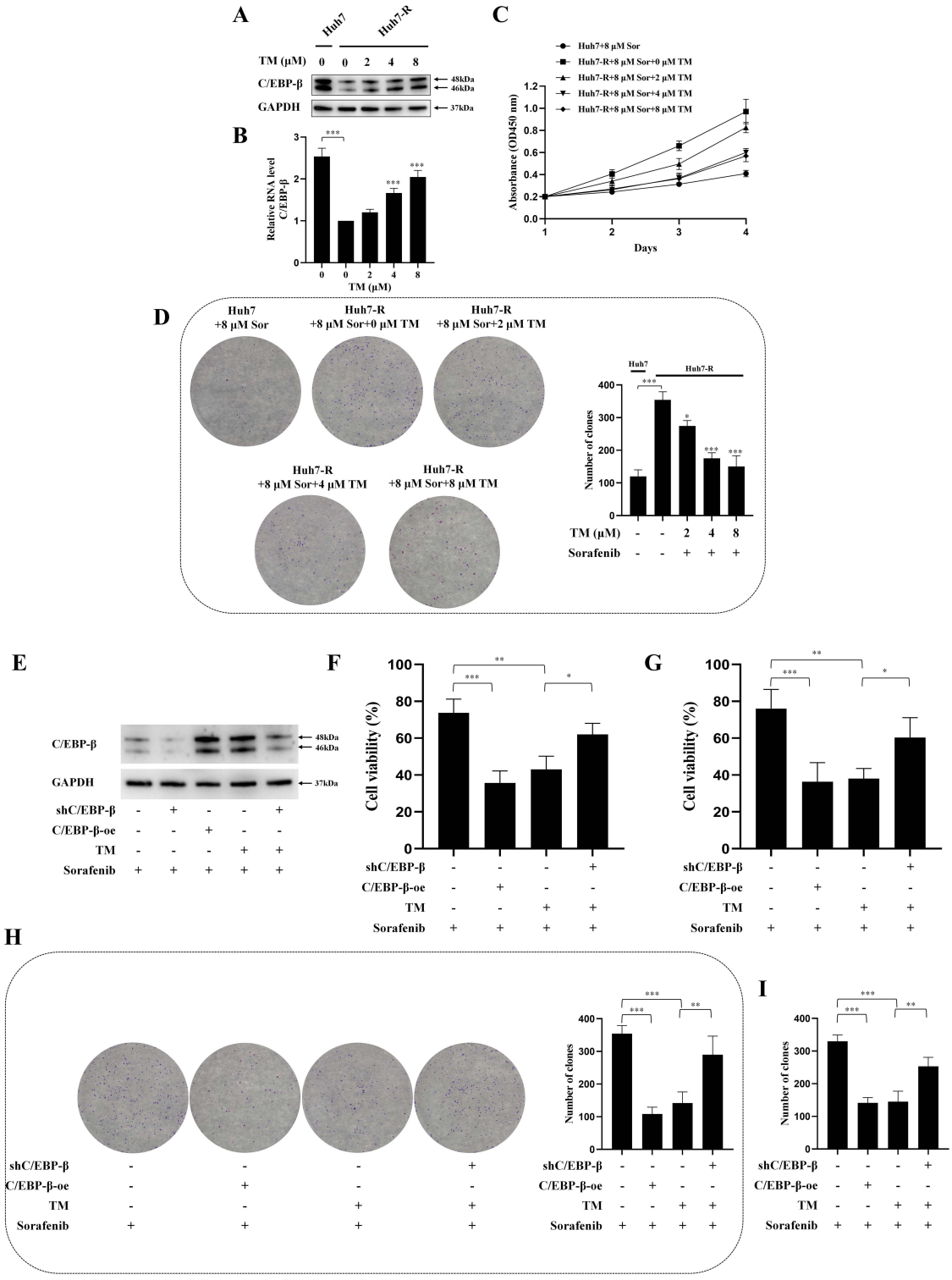

Figure 2 Tunicamycin (TM) reverses sorafenib resistance by upregulating C/EBP-β. (**A**) Western blot analysis of C/EBP-β protein levels in parental Huh7 and resistant Huh7-R cells treated with increasing concentrations of TM (0, 2, 4, 8 μM) for 48 h. (**B**) RT-qPCR analysis of relative C/EBP-β mRNA levels in cells treated as in (**A**). (**C**) Cell viability of Huh7-R cells was measured by CCK-8 assay. Cells were treated with 8 μM sorafenib alone or in combination with TM (2, 4, 8 μM) for the indicated durations. Parental Huh7 cells treated with 8 μM sorafenib served as a sensitive control. (**D**) Clonogenic potential of cells treated as in (**C**). Representative images (left) and quantification (right) are shown. (**E**) Western blot validation of C/EBP-β overexpression (C/EBP-β-oe) and knockdown (shC/EBP-β) in Huh7-R cells under various treatment conditions. (**F**) Cell viability (CCK-8) of genetically modified or unmodified Huh7-R cells treated with sorafenib (8 μM) with or without TM (4 μM) for 48 h. (**G**) Cell viability (CCK-8) of HepG2-R cells treated as in (**F**). (**H**) Clonogenic potential of Huh7-R cells treated as in (**F**). (**I**) Clonogenic potential of HepG2-R cells treated as in (**F**). The "+" and "-" signs indicate the presence or absence of the specified treatment, respectively. All quantitative data are presented as mean ± SD from three independent experiments. $^{*}P < 0.05$, $^{**}P < 0.01$, and $^{***}P < 0.001$ compared between indicated groups.

https://doi.org/10.2147/JHC.S587037

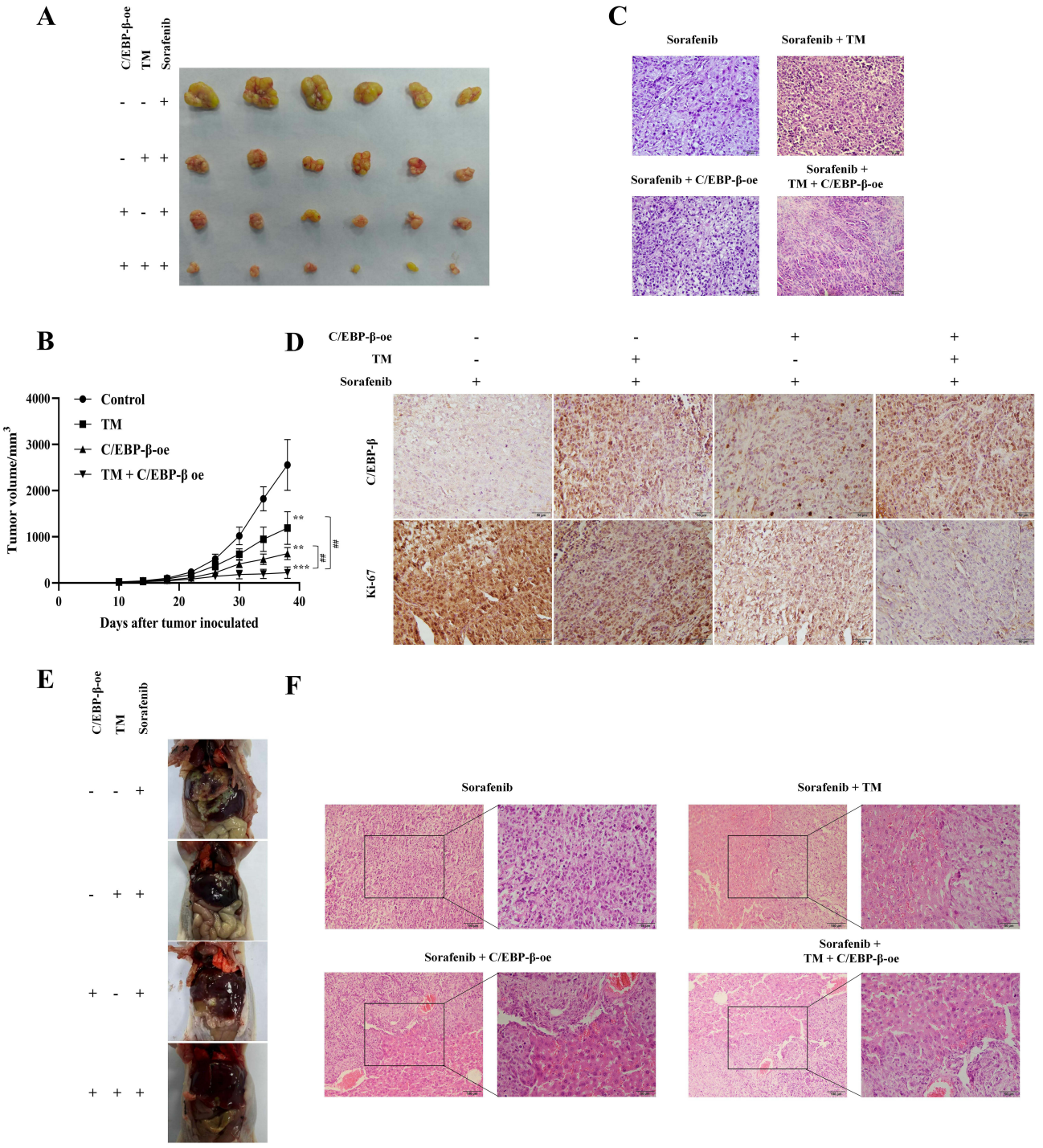

Figure 3 TM and C/EBP-β overexpression cooperatively suppress sorafenib-resistant tumor growth in vivo. Nude mice were treated with sorafenib (15 mg/kg/day) alone (control), sorafenib plus tunicamycin (TM, 0.04 mg/kg/day), sorafenib plus C/EBP-β overexpression (C/EBP-β-oe), or a combination of sorafenib, TM, and C/EBP-β-oe. (**A**–**D**) Subcutaneous xenograft model using Huh7-R cells. (**A**) Representative images of excised tumors from each treatment group on day 38. (**B**) Tumor growth curves measured over a 38-day treatment period. Data are presented as mean ± SD (n=6 mice per group). $^{**}P<0.01$ and $^{***}P<0.001$ compared with the sorafenib-only group. $^{\#\#}P<0.01$ compared between indicated groups. (**C**) H&E staining of tumor sections showing tumor morphology and cell density. Scale bars, 50 μm. (**D**) Immunohistochemical staining for C/EBP-β and proliferation marker Ki-67 in tumor tissues. Scale bars, 50 μm. (**E** and **F**) Orthotopic xenograft model of Huh7-R cells. (**E**) Representative images of the liver illustrating intrahepatic tumor burden at the experimental endpoint. (**F**) Representative H&E staining of liver sections from the orthotopic model, with insets providing magnified views of tumor foci. Scale bars: 100 μm (main) and 50 μm (inset). The "+" and "-" signs indicate the presence or absence of the specified treatment, respectively.

https://doi.org/10.2147/JHC.S587037

The C/EBP-β-ROS Axis Is Essential for Tunicamycin-Induced Apoptosis and the Reversal of Sorafenib Resistance

To elucidate the molecular mechanisms underlying the re-sensitization of sorafenib-resistant cells, we investigated the interplay between oxidative stress and apoptosis downstream of TM treatment and C/EBP-β modulation. First, intracellular reactive oxygen species (ROS) levels were assessed via DCFDA staining. Hydrogen peroxide (H_2O_2) was utilized as a positive control, which, as expected, induced the strongest ROS accumulation. Compared to the sorafenib-only control, both TM administration and C/EBP-β overexpression (C/EBP-β-oe) induced a significant accumulation of intracellular ROS. Notably, this TM-induced ROS surge was markedly attenuated by C/EBP-β knockdown (shC/EBP-β) and effectively abolished by the ROS scavenger N-acetylcysteine (NAC), substantiating the C/EBP-β-dependency of this oxidative stress (Figure 4A and B). Functionally, TUNEL assays demonstrated that both TM and C/EBP-β-oe triggered a dramatic increase in apoptosis. This pro-apoptotic effect was significantly mitigated by either C/EBP-β silencing or NAC co-treatment, proving that ROS generation is a prerequisite for apoptosis (Figure 4C and D). To dissect the signaling cascade, we performed Western blot analysis (Figure 4E). While both TM and C/EBP-β-oe upregulated the tumor suppressor p53, this upregulation was reversed by shC/EBP-β but remained unaffected by NAC. This suggests that p53 activation functions either upstream of or in parallel to ROS production, rather than as a downstream effector. Similarly, the TM-induced upregulation of C/EBP-β was entirely unaffected by NAC treatment, confirming its upstream role. Conversely, both interventions significantly elevated the pro-apoptotic Bax/Bcl-2 ratio and cleaved caspase-3 levels. Importantly, the activation of this executioner caspase cascade by TM was largely abrogated by both C/EBP-β knockdown and ROS scavenging. Collectively, these data delineate a synergistic mechanistic axis: while resistant cells can tolerate basal sorafenib treatment, TM induces a C/EBP-β-dependent surge in intracellular ROS. This severe oxidative stress overwhelms the cellular antioxidant defenses, synergizing with sorafenib to forcefully drive the intrinsic apoptotic pathway and overcome sorafenib resistance.

Integrated Bioinformatic Analyses Reveal a C/EBP-β-Dependent Transcriptomic Program Underlying TM's Efficacy

To further elucidate the molecular mechanisms substantiating our experimental findings, we performed comprehensive bioinformatic analyses. Initially, Gene Set Enrichment Analysis (GSEA) of the TCGA-LIHC cohort was employed to assess clinical relevance. The analysis revealed that elevated C/EBP-β expression is positively correlated with critical apoptosis and endoplasmic reticulum (ER) stress signatures, specifically the TWEAK signaling pathway and ATF4-mediated ER stress gene activation (Figure 5A). Subsequently, we screened for potential therapeutic targets of TM. By intersecting predicted drug targets (sourced from SwissTargetPrediction, PharmMapper, and DrugBank) with HCC-associated genes (curated from GeneCards and OMIM), we identified 185 candidate genes (Figure 5B and Table S1). To delineate the biological functions of these candidates, we performed Gene Ontology (GO) and Kyoto Encyclopedia of Genes and Genomes (KEGG) enrichment analyses. The results demonstrated a marked enrichment in apoptotic processes, including the "intrinsic apoptotic signaling pathway" and "regulation of apoptotic signaling pathway". Notably, the enrichment of terms such as "response to oxygen levels" and "response to hypoxia" aligns with our in vitro observations of TM-induced ROS accumulation. Collectively, these findings suggest that the therapeutic efficacy of TM in HCC is mediated through the activation of cell death programs intrinsically linked to oxidative stress (Figure 5C). Finally, to pinpoint the convergent mechanism, we intersected the TM targets with known C/EBP-β-regulated genes, isolating a core set of 13 targets. Functional interrogation of this gene set revealed a specific enrichment in the "intrinsic apoptotic signaling pathway in response to endoplasmic reticulum stress", alongside multiple cell differentiation pathways (Figure 5D).

Discussion

Acquired resistance significantly limits the clinical efficacy of sorafenib in advanced hepatocellular carcinoma (HCC). During HCC progression, particularly under continuous therapeutic pressure, adaptive endoplasmic reticulum (ER) stress is often engaged to promote tumor survival. Interestingly, our resistant models revealed a marked

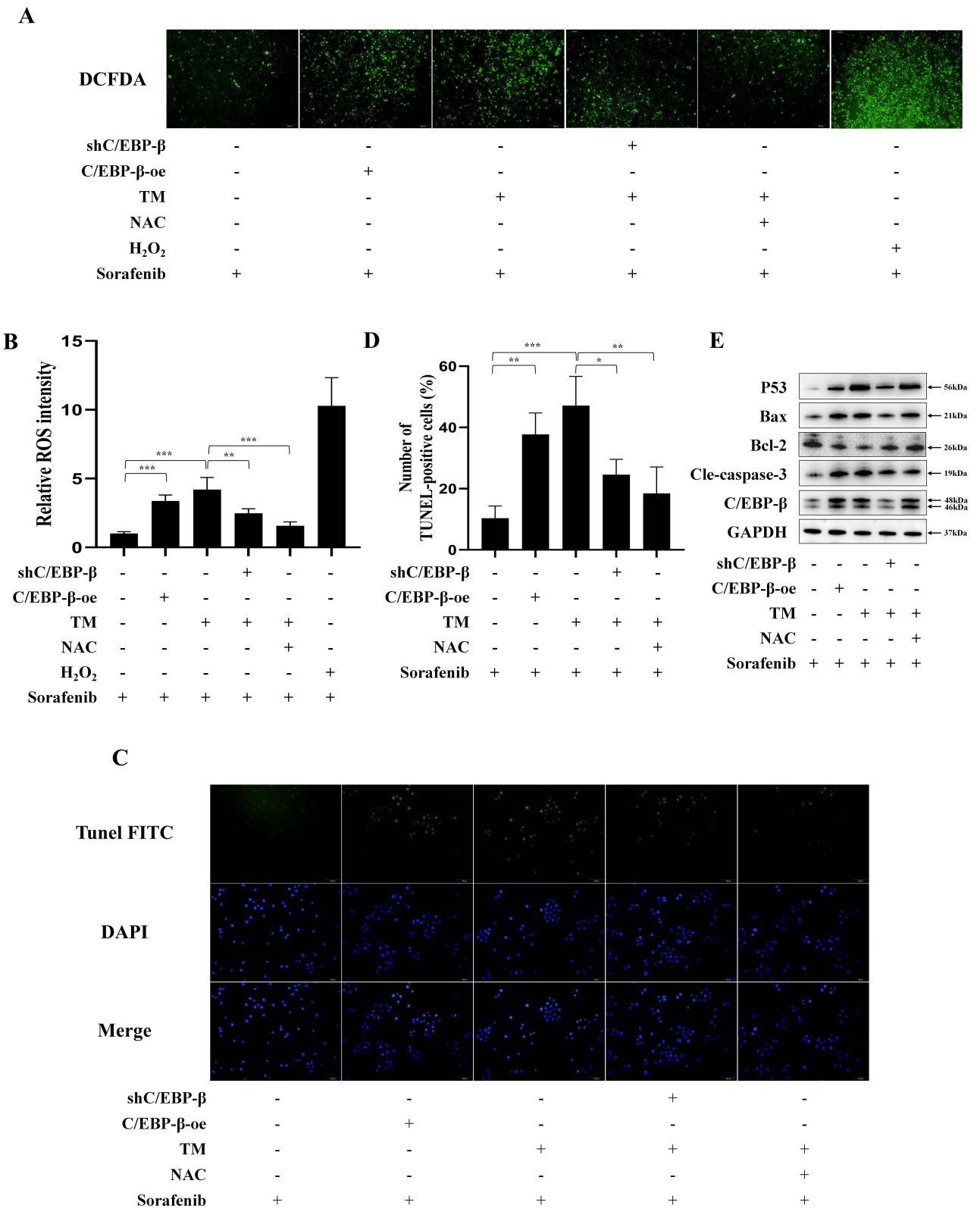

Figure 4 The C/EBP-β axis overcomes sorafenib resistance by inducing ROS production and apoptosis in Huh7-R cells. Huh7-R cells were treated for 48 h with sorafenib (8 μM) alone or in combination with C/EBP-β overexpression (C/EBP-β-oe), tunicamycin (TM, 4 μM), TM plus shC/EBP-β, or TM plus NAC (5 mM). Hydrogen peroxide (H_2O_2, 2 mM) was included as a positive control for ROS generation. (**A**) Intracellular ROS levels were detected using DCFDA staining and visualized using fluorescence microscopy. Scale bar, 200 μm. (**B**) Quantification of the relative fluorescence intensity from (**A**). (**C**) Apoptosis was detected using the TUNEL assay, with TUNEL-positive nuclei stained green and all nuclei counterstained with DAPI (blue). Scale bar, 100 μm. (**D**) Percentage of TUNEL-positive cells from (**C**). (**E**) Western blot analysis of C/EBP-β, p53, Bax, Bcl-2, and cleaved caspase-3 protein levels. GAPDH was used as an internal control. The "+" and "-" signs indicate the presence or absence of the specified treatment, respectively. All quantitative data are presented as mean ± SD from three independent experiments. **P* < 0.05, ***P* < 0.01, and ****P* < 0.001 compared between indicated groups.

 https://doi.org/10.2147/JHC.S587037

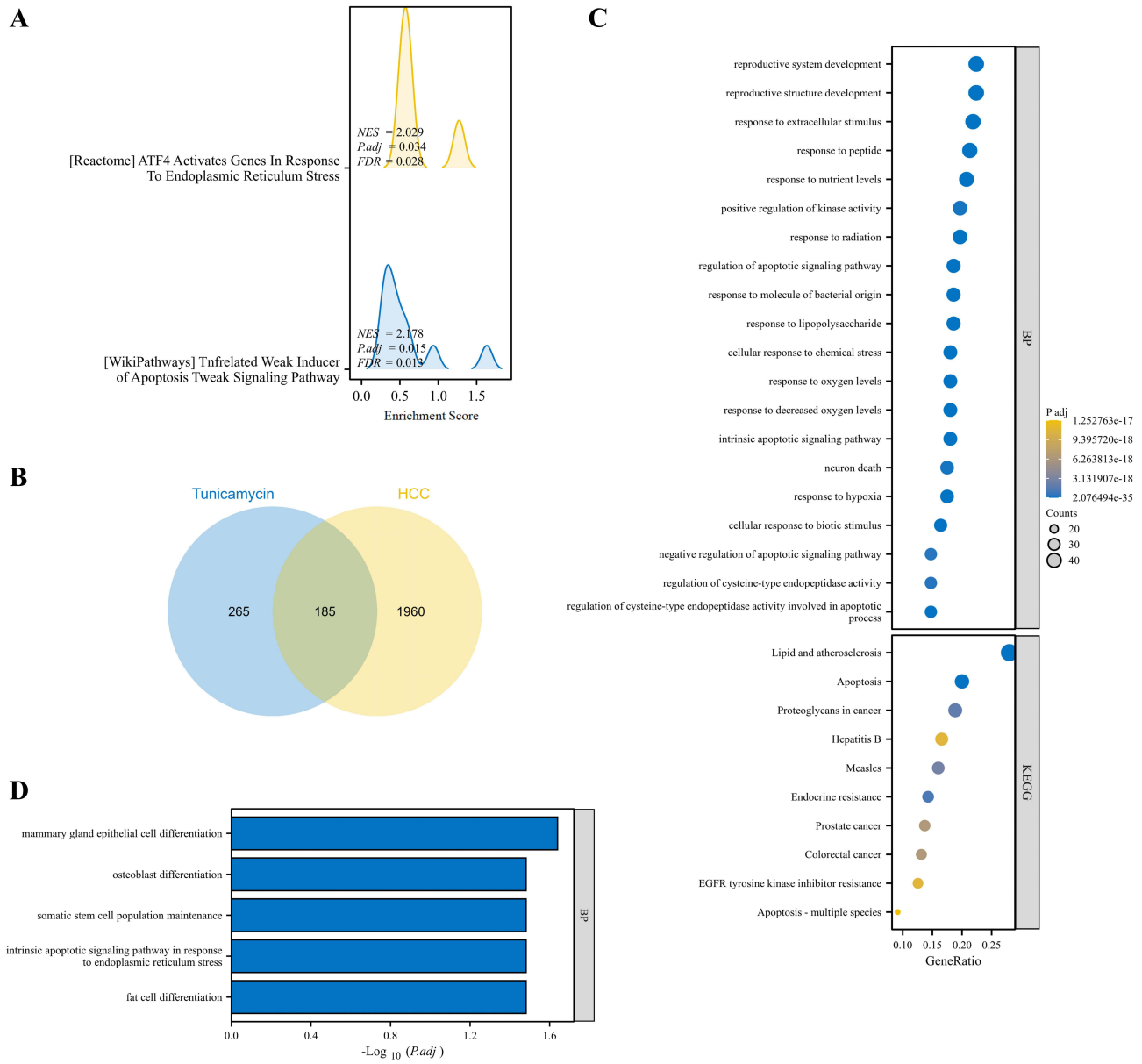

Figure 5 Integrated bioinformatic analyses define the C/EBP-β-dependent transcriptomic mechanism of tunicamycin in HCC. (**A**) Representative Gene Set Enrichment Analysis (GSEA) plots from the TCGA-LIHC dataset showing positive enrichment of apoptosis (TWEAK signaling) and ER stress (ATF4 activation) pathways in tumors with high C/EBP-β expression. (**B**) Venn diagram illustrating the identification of 185 intersecting genes between potential Tunicamycin (TM) targets (from SwissTarget, Pharmmapper, and DrugBank) and known hepatocellular carcinoma (HCC) disease genes (from GeneCards and OMIM). (**C**) GO (Biological Process) and KEGG pathway enrichment analysis of the 185 intersecting genes identified in (B). The bubble plot displays top enriched terms, with bubble size corresponding to gene count and color intensity reflecting the adjusted *P*-value. (**D**) GO enrichment analysis (Biological Process) of the 13 core genes at the intersection of TM's potential targets and C/EBP-β-regulated differentially expressed genes. The bar chart highlights "intrinsic apoptotic signaling pathway in response to ER stress" and "multiple cell differentiation-related pathways" as the key convergent mechanisms.

downregulation of C/EBP-β, a downstream effector of the ER stress response. This suggests a plausible mechanism: resistant cells may adaptively bypass stress-induced apoptosis by suppressing pro-apoptotic effectors like C/EBP-β, thereby maintaining a survival advantage and driving the resistant phenotype. Building on our previous work establishing that C/EBP-β synergizes with sorafenib to suppress HCC growth, we hypothesized that pharmacologically pushing ER stress beyond the cellular adaptive threshold could overcome this resistance. To achieve this, we utilized a sufficient concentration of tunicamycin (TM), a potent N-linked glycosylation inhibitor that triggers severe, unresolvable ER stress rather than a mild adaptive response. We demonstrated that TM exhibits robust therapeutic effectiveness in HCC by upregulating C/EBP-β, essentially dismantling the adaptive survival

https://doi.org/10.2147/JHC.S587037

mechanisms of resistant cells and restoring sorafenib sensitivity in vitro and in vivo. To the best of our knowledge, this is the first report to demonstrate that pharmacological hyperactivation of ER stress reverses acquired sorafenib resistance specifically by restoring C/EBP-β signaling. While the induction of apoptosis via ER stress is generally recognized as a promising antitumor strategy,[13,14] our functional assays delineate how TM synergizes with sorafenib: while resistant cells can successfully evade the baseline kinase-inhibitory effects of sorafenib monotherapy, TM launches a massive, C/EBP-β-dependent surge of intracellular ROS. This combined dual assault completely overwhelms the cellular antioxidant defenses, simultaneously halting tumor growth and forcefully driving the intrinsic apoptotic cascade.[15,16]

While we confirmed that C/EBP-β is a critical mediator, the loss-of-function experiments showed that C/EBP-β knockdown only partially reversed the sensitizing effect of TM. This incomplete rescue suggests the involvement of parallel, C/EBP-β-independent mechanisms. The bioinformatics analysis and literature review point to the PERK-eIF2α-ATF4-CHOP signaling pathway as a likely co-conspirator. CHOP (DDIT3), a canonical pro-apoptotic transcription factor, is often co-regulated with C/EBP-β under severe stress.[12,17] It is highly probable that TM-induced ATF4 simultaneously upregulates both CHOP and C/EBP-β, which may act synergistically to execute the apoptotic program. This multi-pathway activation explains why blocking C/EBP-β alone was insufficient to completely abolish the therapeutic effect of TM. Beyond apoptosis, our bioinformatics analysis revealed that TM/C/EBP-β co-regulated genes are highly enriched in cellular differentiation pathways. This raises an intriguing possibility that C/EBP-β may concurrently suppress the "stemness" traits typically associated with HCC drug resistance,[18] thereby attacking the resistant phenotype from multiple angles.

Intriguingly, the massive accumulation of intracellular ROS observed in our study suggests that the therapeutic mechanism of the TM-C/EBP-β axis may extend beyond classical apoptosis. Recent high-impact studies have highlighted that inducing ferroptosis—an iron-dependent form of cell death driven by ROS-mediated lipid peroxidation—is a potent strategy to overcome sorafenib resistance in HCC.[19,20] Although the current study focused on the apoptotic pathway, elevated ROS is also a prerequisite for ferroptosis. Exploring whether C/EBP-β modulates oxidative stress to influence other cell death modalities, such as ferroptosis, represents a compelling direction for our future research.

Regarding clinical translation, it is essential to address the current status of tunicamycin. Although TM is a potent experimental tool for inducing ER stress, its clinical application has been hampered by significant toxicity concerns and a narrow therapeutic window, preventing it from entering advanced clinical trials.[21,22] Therefore, the clinical value of our study lies not in proposing TM as a direct drug, but in validating the "ER stress-C/EBP-β-ROS" axis as a druggable vulnerability. Future drug development should focus on identifying safer ER stress inducers or specific small-molecule activators of C/EBP-β that can mimic the sensitizing effects of TM without its systemic toxicity.

Finally, we must acknowledge several limitations of this study. First, our conclusions are based on data from only two HCC cell lines (Huh7-R and HepG2-R) and their derived xenografts; we did not include primary patient-derived tumor samples, which would better reflect the heterogeneity of clinical HCC.[23] Second, while we observed significant tumor regression in vivo, we did not perform a comprehensive toxicology assessment to evaluate the systemic side effects of the TM-sorafenib combination.[24] Future investigations will need to address these gaps and further explore the precise molecular interplay between C/EBP-β and the PERK-eIF2α-ATF4-CHOP signaling pathway.

In summary, this study identifies C/EBP-β as a pivotal target for reversing acquired sorafenib resistance in hepatocellular carcinoma. We demonstrate that Tunicamycin (TM) restores drug sensitivity specifically by triggering the C/EBP-β-ROS-intrinsic apoptosis signaling axis. These findings suggest a novel clinical approach: incorporating ER stress inducers or developing specific C/EBP-β activators could serve as effective adjuvants to overcome resistance in HCC patients.

Data Sharing Statement

The raw data and analytical materials supporting the conclusions of this article are available from the corresponding author upon reasonable request.

Ethics Declarations

All animal experiments were approved by the Chengde Medical College Animal Care and Use Committee (Approval No. CDMULAC-20241104-051) and were conducted strictly in accordance with the American Veterinary Medical Association (AVMA) Guidelines for the Euthanasia of Animals.

Consent for Publication

The authors consented to the publication.

Acknowledgments

This work was funded by the Natural Science Foundation of Hebei Province (Grant No. H2021406043), Open Project of the Key Laboratory of Traditional Chinese Medicine Research and Development of Hebei Province (Grant No. ZSKF202303), Medical Science Research Project of Hebei Provincial Health Commission (Grant No. 20260702), School-level research project of Chengde Medical University (Grant No. 201613), and the key discipline of neurobiology of Chengde Medical University (071006).

Author Contributions

Chong Pang and Jian Chen are co-first authors. All authors made a significant contribution to the work reported, whether that is in the conception, study design, execution, acquisition of data, analysis and interpretation, or in all these areas; took part in drafting, revising or critically reviewing the article; gave final approval of the version to be published; have agreed on the journal to which the article has been submitted; and agree to be accountable for all aspects of the work.

Disclosure

The authors declare no competing interests.

References

1. Xia S, Pan Y, Liang Y, Xu J, Cai X. The microenvironmental and metabolic aspects of sorafenib resistance in hepatocellular carcinoma. *EBioMedicine*. 2020;51:102610. doi:10.1016/j.ebiom.2019.102610
2. Jiang X, Ge X, Huang Y, et al. Drug resistance in TKI therapy for hepatocellular carcinoma: mechanisms and strategies. *Cancer Lett*. 2025;613:217472. doi:10.1016/j.canlet.2025.217472
3. Xu J, Wang B, Liu Q, et al. MVP-LCN2 axis triggers evasion of ferroptosis to drive hepatocarcinogenesis and sorafenib resistance. *Drug Resist Updat*. 2025;81:101246. doi:10.1016/j.drup.2025.101246
4. Tang W, Chen Z, Zhang W, et al. The mechanisms of sorafenib resistance in hepatocellular carcinoma: theoretical basis and therapeutic aspects. *Signal Transduct Target Ther*. 2020;5(1):87. doi:10.1038/s41392-020-0187-x
5. Wei M, Cao Z, Dong L, et al. The advantages and challenges of sorafenib combination therapy: drug resistance, toxicity and future directions (Review). *Oncol Lett*. 2025;30(5):526. doi:10.3892/ol.2025.15272
6. Yin YC, He J, Feng Y, et al. FiLactate-induced lysine lactylation: a central node linking metabolic rewiring, epigenetic plasticity and therapeutic vulnerabilities in hepatocellular carcinoma. *J Biochem Mol Toxicol*. 2025;39(12):e70622. doi:10.1002/jbt.70622
7. Li M, Duan M, Yang Y, et al. Combination of brefeldin A and tunicamycin induces apoptosis in HepG2 cells through the endoplasmic reticulum stress-activated PERK-eIF2α-ATF4-CHOP signaling pathway. *Liver Res*. 2025;9(1):49–56. doi:10.1016/j.livres.2025.01.004
8. Shi TL, Zhang L, Cheng QY, et al. Xanthatin induces apoptosis by activating endoplasmic reticulum stress in hepatoma cells. *Eur J Pharmacol*. 2019;843:1–11. doi:10.1016/j.ejphar.2018.10.041
9. Arensdorf AM, Rutkowski DT. Endoplasmic reticulum stress impairs IL-4/IL-13 signaling through C/EBPβ-mediated transcriptional suppression. *J Cell Sci*. 2013;126(Pt 17):4026–4036. doi:10.1242/jcs.130757
10. He A, Wu C, Xia D, Zhu Y. CEBPB emerges as a key regulatory factor in human cancers through diverse molecular mechanisms and clinical implications. *Discov Oncol*. 2025;16(1):2278. doi:10.1007/s12672-025-04122-6
11. Pang C, Miao H, Zuo Y, Guo N, Sun D, Li B. C/EBPβ enhances efficacy of sorafenib in hepatoblastoma. *Cell Biol Int*. 2021;45(9):1897–1905. doi:10.1002/cbin.11624
12. Yang X, Du T, Wang X, et al. IDH1, a CHOP and C/EBPβ-responsive gene under ER stress, sensitizes human melanoma cells to hypoxia-induced apoptosis. *Cancer Lett*. 2015;365(2):201–210. doi:10.1016/j.canlet.2015.05.027
13. Bhardwaj A, Panepinto MC, Ueberheide B, Neel BG. A mechanism for hypoxia-induced inflammatory cell death in cancer. *Nature*. 2025;637(8045):470–477. doi:10.1038/s41586-024-08136-y
14. Yang J, Chen F, Fu Z, Yang F, Saba NF, Teng Y. Blocking the TCA cycle in cancer cells potentiates CD36+ T-cell-mediated antitumor immunity by suppressing ER stress-associated THBS2 signaling. *Cancer Res*. 2025;85(11):2014–2026. doi:10.1158/0008-5472.CAN-24-3477
15. Saint-Auret G, Danan JL, Hiron M, et al. Characterization of the transcriptional signature of C/EBPbeta isoforms (LAP/LIP) in Hep3B cells: implication of LIP in pro-survival functions. *J Hepatol*. 2011;54(6):1185–1194. doi:10.1016/j.jhep.2010.09.021

16. Maehara O, Ohnishi S, Asano A, et al. Metformin regulates the expression of CD133 through the AMPK-CEBPβ pathway in hepatocellular carcinoma cell lines. *Neoplasia*. 2019;21(6):545–556. doi:10.1016/j.neo.2019.03.007
17. Wen J, Xuan B, Gao Y, et al. Lnc-17Rik promotes the immunosuppressive function of Myeloid-Derived suppressive cells in esophageal cancer. *Cell Immunol*. 2023;385:104676. doi:10.1016/j.cellimm.2023.104676
18. Thunen A, La Placa D, Zhang Z, Shively JE. Role of lncRNA LIPE-AS1 in adipogenesis. *Adipocyte*. 2022;11(1):11–27. doi:10.1080/21623945.2021.2013415
19. Elmetwalli A. Ferroptosis and the cGAS-STING pathway into precision nano-immuno-theranostics: a mechanistic paradigm for reversing drug resistance in hepatocellular carcinoma. *Drug Resist Updat*. 2026;84:101326. doi:10.1016/j.drup.2025.101326
20. Ladd AD, Duarte S, Sahin I, Zarrinpar A. Mechanisms of drug resistance in HCC. *Hepatology*. 2024;79(4):926–940. doi:10.1097/HEP.0000000000000237
21. Kurosu M, Mitachi K. DPAGT1-perspective as an anticancer drug target. *Molecules*. 2025;30(20):4049. doi:10.3390/molecules30204049
22. Nghiem TT, Nguyen KA, Kusuma F, et al. The PERK-eIF2α-ATF4 axis is involved in mediating ER-stress-induced ferroptosis via DDIT4-mTORC1 inhibition and acetaminophen-induced hepatotoxicity. *Antioxidants*. 2025;14(3):307. doi:10.3390/antiox14030307
23. Zhang Z, Zhang Z, Zhang Y, et al. Phosphoproteomics delineates hepatocellular carcinoma subtypes and pinpoints therapeutic targets. *Hepatology*. 2025;82(6):1432–1449. doi:10.1097/HEP.0000000000001250
24. Xu Z, Huang X, Su Q, et al. Flemiphilippinin A induces paraptosis in lung cancer cells via c-Myc-driven endoplasmic reticulum stress and CHOP-mediated mitochondrial dysfunction. *Phytomedicine*. 2025;146:157098. doi:10.1016/j.phymed.2025.157098